Effect of Alginate Additives on the Microstructure and Properties of Phytic Acid-based Conversion Coating on a Steel Surface

Yong Lu[1,2,], Huixia Feng[1]*

[1] School of Petrochemical Engineering,Lanzhou University of Technology,Lanzhou,Gansu China
[2] Research Institute of Lanzhou Petrochemical Corporation of Petrochina,Lanzhou,Gansu China
[*]E-mail: luyong19850627@163.com

Phytic acid (PA) has a potential use as a coating on metal surface to retard corrosion. However, a loose structure and micro-cracks in the phytic acid coating layer damage the tightness of the coating, providing channels for the infiltration of corrosive media and seriously weakening the protective effect of the coating. Sodium alginate (SA) was added as an accelerating agent to improve the anti-corrosion protective effect and coating densification of the phytic acid coating on a Q235 steel surface. The micro-morphology, elemental composition and elemental chemical state of different samples were observed by the surface analysis technologies of scanning electron microscopy (SEM) equipped with X-ray energy dispersive spectrum (EDS) and X-ray photoelectron spectroscopy (XPS), all of which show a dense and homogenous phytic acid film with lower crack was precipitated on the sample treated by PA-SA conversion coating. Atomic force microscopy (AFM) and contact angle measurements were used to evaluate the adhesion properties of the prepared coating and the results showed that the PA-SA coated steel exhibited better wettability and adhesion to the top layers compared to the bare steel and phytic acid coating. The electrochemical measurements show that the corrosion resistance of the conversion coating was markedly improved on the steel substrate treated by phytic acid conversion bath containing SA.

1. INTRODUCTION

Chemical conversion coating technology is widely used for metal surface treatment which can provide good anti-corrosion protection and further improve the adhesion ability to the subsequent coating layer. These coating technologies are involved in automobile and household appliance manufacturing, hardware processing and many other industries.

Chromate and phosphate is the most widely used kinds of chemical conversion film-formingmaterial. But those are gradually banned because of its lasting harm to the environment. The development and application of green environment-friendly metal surface pretreatment technology has become a very important research direction in the field of metal surface treatment. Through the efforts of the scientific research personnel, have developed a kind of environment-friendly conversion coating. Phytic acid is a natural, nontoxic, multifunctional organic macromolecule that can dissolve in water and widely exists in legumes, such as corn, soybeans and nuts. That contains six phosphate groups giving them a powerful chelating capability to form stable metal-phytic complexes over a wide range of pH values with variety of metallic ions, such as Fe^{2+}, Fe^{3+}, Mg^{2+}, Ca^{2+} and Zn^{2+} [1]. Phytic acid conversion coatings contain abundant hydroxyl groups and phosphate groups that can effectively chemically crosslink with the organic coating and significantly enhance adhesion to the subsequent layer. Nevertheless, some micro-cracks formed in the phytic acid based coating and that cannot provide preferable corrosion resistance for the steel substrate. Further promotion and application of phytic acid conversion coatings are extremely restricted to the field of metal surface treatment [2-3]. The performance of the conversion coating mainly depends on its continuity and thickness. Cracks damage the tightness of the coating and provide an efficient channel for corrosive medium to enter, seriously weakening the protective effect of the coating. In a corrosive environment, corrosive ions and water molecules can migrate and diffuse through the cracks to reach the substrate more easily. This leads to decreased adhesion and delamination of the coating, which is one of the main failure mechanism of coating [4].

To improve the protective capabilities of conversion coatings, various additives were mixed into the preparation process or the conversion coating was post-treated to enhance corrosion resistance. Additives include metal ions [5-6], nano-particles [7-8] and accelerants, such as polyvinyl alcohol and citric acid [9-12]. The different additives in the conversion solution have different densification mechanisms for the formed coating. Metal ions are usually added in a bath with phosphate groups such as phosphoric acid or phytic acid because phosphate groups and metal ions can bond to form complexes. Nano-particles are also commonly found in phosphate conversion films and their main function is to facilitate the formation of phosphate crystals. Accelerants can be used in the densification process of phosphates or rare earth salt conversion films. Polyvinyl alcohol affects the nucleation process of phosphates and their formation of complexes with metal ions, while the role of polyvinyl alcohol in cerium salts is mainly due to the formation of complexes with Ce^{3+} chelating. Citric acid is used in the cross-linking of rare earth salts in conversion coating. Post-treatments include hydrophosphate [13-14], sol-gel [15-16], composite conversion films [17-18] and other post-treatment techniques [19-20]. It can be surmised that other organics which contain functional groups can form complexes with metallic ions could be applied to optimize the densification of conversion coatings. To the best of our current knowledge, there has been relatively little scientific study regarding the properties of conversion coatings when sodium alginate is added to the phytic acid conversion bath. Sodium alginate is a carbohydrate biopolymer $[(C_6H_7Na_{1/2}O_6)n]$ and it exhibits good corrosion protection for aluminium [21], magnesium [22], carbon steel [23] and mild steel [24].

In the present work, we investigated the effect of sodium alginate on the morphology, corrosion resistance and adhesion properties of phytic acid-based conversion coatings on Q235 steel. The

morphological and surface characteristics of the coatings were characterized by the surface analysis technologies of SEM-EDS, XPS, AFM and contact angle measurements, respectively. Furthermore, the corrosion behaviour of the coated Q235 steel was evaluated through electrochemical impedance spectroscopy (EIS) and polarization curves in a 3.5wt.% NaCl electrolyte solution.

2.EXPERIMENTAL

2.1 Materials and coating preparation

All reagents were of analytical grade. Phytic acid (PA) was provided by Aladdin Biochemical Technology Co.Ltd. Sodium chloride was provided by Sinopharm chemical reagent Co.Ltd. Sodiumhydroxide was used to adjust pH values and was provided by Yantai ShuangShuang Chemical Co.Ltd. Sodium alginate (SA) was provided by Tianjin GuangfuFine Chemical Research Institute.

Electrochemical tests were performed using Q235 steel measuring 10×10×4mm prepared by China National Chemical Corporation and the main compositions (wt.%) are listed in Table 1. The steel sheets were polished with a series of emery papers (400, 600, 800, 1000, 1500 and 2000 grit) and then ultrasonically rinsed in anhydrous ethanol and acetone, successively, for 10 min.

Table 1. Chemical compositions of Q235 steel (wt.%)

Element	C	Mn	Si	S	P	Fe
Composition wt%	0.17	0.46	0.46	0.017	0.05	balance

2.2 Fabrication of conversion coating

The phytic acid conversion coating was prepared in 20 g/L phytic acid solution at 60°C for 20 min in the absence and in the presence of different concentrations of sodium alginate. The pH of the phytic acid bath was finally fixed at 5. After the conversion process, the samples were thoroughly rinsed with deionized water and dried in cold air for 2 h. The compositions of the phytic acid baths are described in Table 2.

Table 2. Conversion baths with different concentration of SA (marked as PA-SA)

Label	Composition g/L	
	Phytic acid	Sodium alginate
Bare steel	—	—
PA coating	20	—
PA-SA-1	20	0.15
PA-SA-2	20	0.30
PA-SA-3	20	0.50
PA-SA-4	20	0.80

Additionally, the corresponding phytic acid iron powder was synthesized to determine the chemical bonding mode of the phytic acid conversion coating on steel. Mainly including: (1) iron powders was added to the above phytic acid solution to obtain the iron phytate liquor; (2) the required iron phytate powder was obtained by drying the liquor at 60°C.

2.3 Surface analysis and characterization

The micro-morphology and the elemental composition of the samples treated by the different baths were examined via SEM (Hitachi JSM-5600LV, JEOL, Japan) equipped with EDS. The elemental chemical states of the coating were probed using XPS (Thermo, ESCALAB 250Xi, USA) with an Al Kα (hν=1486.6eV) monochromatic source, and all spectra were corrected using the signal of C1s at 284.8eV. Curve fitting of the XPS spectra was implemented using a nonlinear least squares curve-fitting program (XPSPEAK 4.1).The surface roughness of coated steel samples was evaluated by an AFM (NanoScope IIIa, VEECO, USA), and contact angle measurements were carried out by a contact angle apparatus (JC2000D3, ShangHai Zhongchen Digtal Technology Apparatus Co., Ltd. China). The thickness of the conversion coating was measured using a coating thickness gauge (DKD-K-33101 DUALSCOPE1MP0R USB, Fischer). Infrared absorption spectra of the iron phytate powder in the absence and in the presence of sodium alginate (marked PA-Fe, and PA-SA-Fe) were measured using FT-IR technique.(FT-IR, Nicolet 5700, USA) in the spectral range $4000 - 400 \text{cm}^{-1}$.

2.4 Electrochemical corrosion measurements

Electrochemical experiments were carried out using a conventional three-electrode cell assembly. Steel sheet was used as the working electrode with an exposed surface area of 1 cm^2 to contact the 3.5 wt% NaCl corrosive solution at 25°C. A platinum sheet was used as the counter electrode and a saturated calomel electrode (SCE) as the reference electrode. Each test was performed using three specimens to ensure the reliability of results. Electrochemical corrosion measurements were conducted using a computer-controlled CHI660E electrochemical workstation. Prior to each measurement, the working electrode was immersed in the electrolyte solution for 30 min to obtain the steady open circuit potential. The EIS measurements were recorded over the frequency spectrum range from 100 kHz to 0.01 Hz, with sinusoidal perturbation of 5mV amplitude at open circuit potential. ZsimpWin soft ware was used to evaluate the parameters obtained by fitting the experimental data. The charge transfer resistance (R_{ct}) values were gained from Nyquist diagrams by measuring the difference in impedance values at low and high frequencies. Polarization testing was implemented at a scanning rate of 0.5 mV/s from −300mV up to +300 mV around open circuit potential.

3. RESULTS AND DISCUSSION

3.1 Characterization of coated samples

3.1.1 Surface morphology analysis

The surface morphology and chemical composition of the coated steel samples were observed using SEM-EDS. The images are shown in Figs.1 and 2.
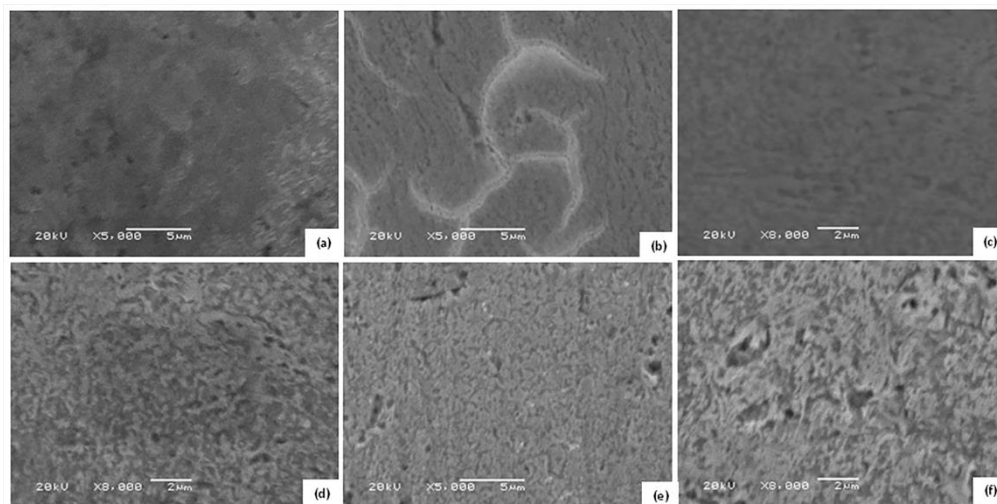
Figure 1. SEM images of different samples. a) not-treated steel, b) PA coated, c) PA-SA-1, d) PA-SA-2, e) PA-SA-3, f) PA-SA-4.
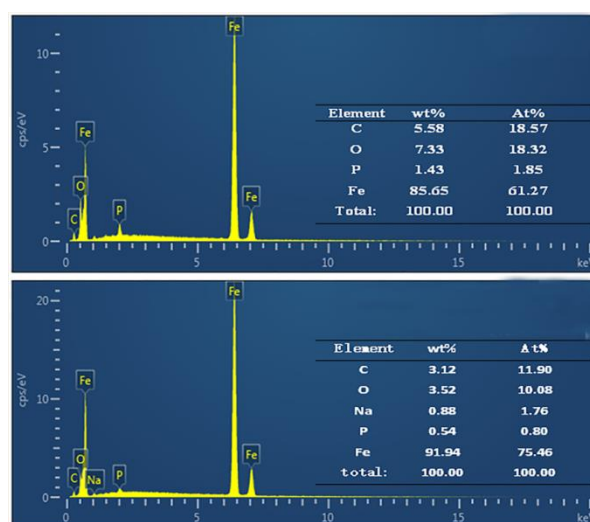
Figure 2. EDS spectra and elemental composition of steel treated with PA (a) and PA-SA-4(b).

Fig. 1 a–f shows the SEM micrographs of the different samples. Based on the Fig 1a, it can be seen that the surface of the polished steel was smooth. Nevertheless, there are some micro-cracks in

the phytic acid-coated sample, which are easily seen. It is clear that SA was added into the phytic acid coating bath resulted in the disappearance of micro-cracks in the coating. Because the sodium alginate molecule is large (between 32000 and 200,000), it may extend into the conversion coating and chelate with iron ions, making the coating more continuous and compact [25]. Moreover, with the increase of SA concentration, flocculation morphology is observed on the steel surface. Fig.2 shows the EDS spectra and elemental composition of the coated samples. As seen in the Fig 2, the phytic acid conversion coating is mainly composed of Fe, C, O and P. And the presence of P in the phytic acid coating enables the phytic acid to better adsorb onto the metal surface to form a chemical conversion coating. The presence of Na on the PA-SA-4 sample demonstrated that sodium alginate may chelate with iron ions or form an adsorbed layer on the steel surface [23]. The film thickness test results demonstrated that the film thickness decreased slightly when sodium alginate was used as an additive. (The thickness of the PA conversion coating reached approximately $5.2 \pm 3\mu m$ but that of PA-SA-4 was only $5.0 \pm 2 \mu m$). It is speculated that when sodium alginate adsorbs onto the steel surface, it slows the dissolution of metallic ions. The concentration of metal ions involved in the chelating reaction was lower than it was before. As a consequence, the thickness of the obtained coating was thinner than the previously obtained coating.

3.1.2 XPS measurements

XPS measurements were performed to estimate the chemical state of the PA-coated substrate. High-resolution XPS spectroscopy allowed a more accurate analysis of surface composition and helped us to detect the chemical state of the surface components. The high-resolution XPS spectra of C 1s, O 1s, P 2p and Fe 2p on the phytic acid-coated sample surfaces are shown in Fig. 3.
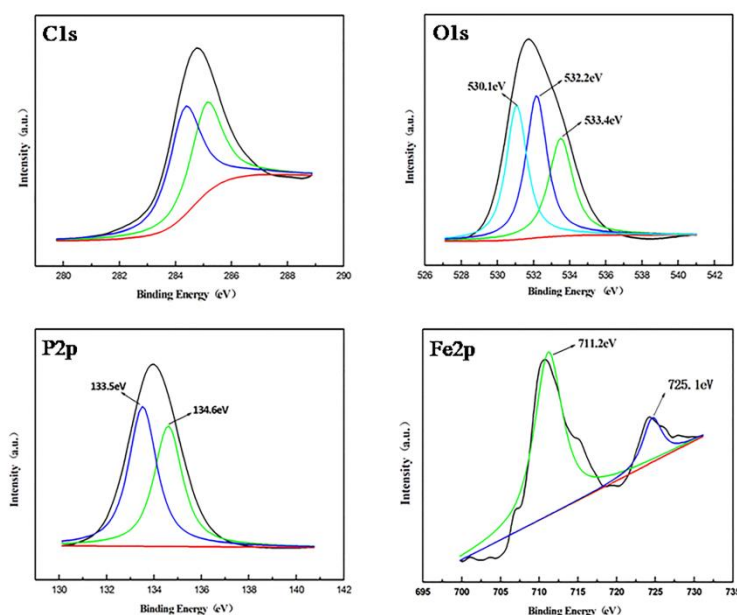
Figure 3. High-resolution spectra of the major elements of the phytic acid coated steel

Due to adventitious hydrocarbons from the environment the presence of carbon is common in XPS surface scans. Other than carbon, the phytic acid conversion coating was composed of P and O, which was consistent with the EDS results. Two deconvoluted peaks at binding energies of 133.5eV and 134.6 eV, were observed in the P 2p spectra of PA-coated steel, corresponding to the chemical states P-O-H and P-O-Fe, respectively [5]. This finding manifests that the phytic acid adsorbed onto the steel surface and formed a thin coating by forming P-O-Fe bonds and verifies the existence of phytic acid on steel surface. The peak of O 1s at about 532.2 eV is assigned to P=O and P-O-Fe structure, a surface metal oxide peak approximately 530.1eV and some adsorbed water peak approximately 533.4eV [15].The Fe 2p region of phytic acid coating contains two peaks, including a large peak appeared at approximately 711.2 eV that corresponds to a ferric-phytic acid complex. This also demonstrates that many P-O-Fe bonds formed during the formation of the coating. A small peak was observed at 725.1 Ev, which can be ascribed to iron oxide (FeOOH), showing that the surface was not completely covered by phytic acid. This demonstrates that the chelating reaction occurred between phytic acid molecules and iron ions. According to observations from the XPS surface analysis of PA coated sample, it can be concluded that phytic acid can form a conversion coating on the steel surface and that was bound to the steel surface through the formation of P-O-Fe(III) [6].

3.1.3 FT-IR analysis
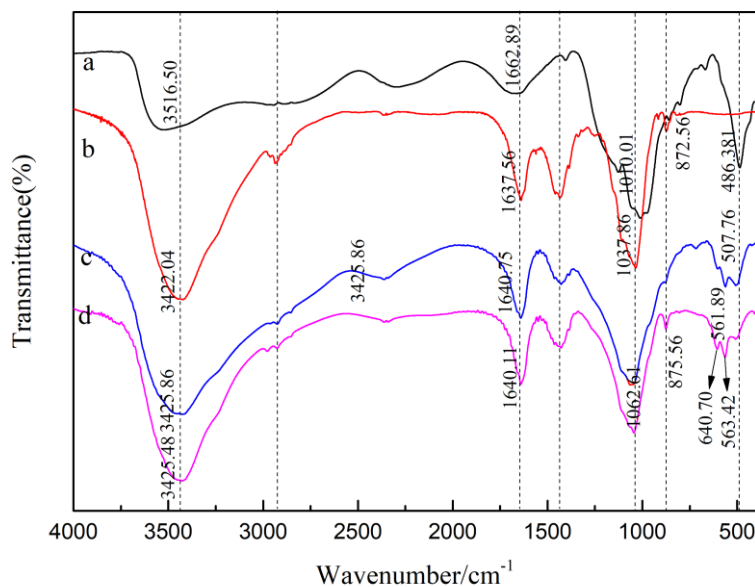
Figure 4. FT-IR spectra of the different samples in the region of 400–4000 cm^{-1} (a: PA, b:SA, c: PA-Fe, d:PA-SA-Fe).

Fig.4 a-d shows the FT-IR spectra of the different samples in the region of 400–4000 cm^{-1}. A series of broad absorption peaks at wave numbers of 3400 cm^{-1}in the FT-IR spectrum were attributed to hydroxyl stretching vibrations. In the FT-IR spectrum of PA (Fig. 4(a)), the characteristic bands of PA are indicated by peaks at 1650 cm^{-1}, 1010.11 cm^{-1} and 486.381 cm^{-1}, corresponding to the

phosphate hydrogen group and phosphate group respectively [26]. For the PA-Fe (Fig. 4(c)), a new peak located at 561.89 cm^{-1} assigned to P–O–Fe bonds emerged, which provided the direct evidences for the formation of metal phytates [27]. For the SA (Fig. 4(b)) and PA-SA-Fe (Fig. 4(d)), peaks around 1637.56 and 1431.18 cm^{-1} were assigned to the asymmetric and symmetric carboxylate bonds. Stretch vibration of the C–O bond were appeared at 1033.87 cm^{-1}. Peaks observed in pure SA confirm the presence of different oxygen–rich functional group constituents in the SA. The iron cations dissolved from the surface of steel are liable to coordinate bonding with oxygen–rich functional group constituents in the SA which provide lone pair electrons. Interestingly, a weak peak appeard at 640 cm^{-1} was attributed to iron–oxygen bond [28], occurred for the iron powder added in the PA–containing SA solution but was obviously missing in pure SA [23].

3.1.4 AFM and surface angle analysis

The nano-scale surface morphology of bare steel and steel treated with PA or PA-SA-4 was studied by AFM (Fig.5).
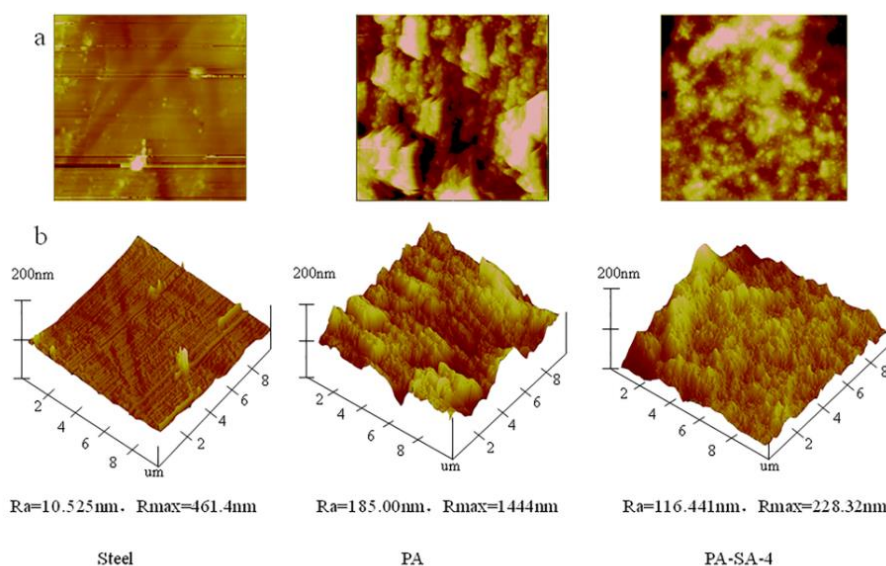
Figure 5. Surface morphology of the steel, PA and PA-SA-4 (a) optical images; (b) AFM images

Fig. 5 shows the nano-scale surface morphology of bare steel and steel treated with PA or PA-SA-4. The untreated steel surface is relatively smooth with obvious scratches resulting from the SiC polishing step. The AFM images in Fig.5b confirm the presence of phytic acid on the steel compared to the bare steel sample. It is evident from the AFM micrographs that the phytic acid deposition on the steel substrate resulted in a marked increase of sample surface roughness (Ra: average roughness and Rmax: the max surface height). The phytic acid-coated steel exhibited a non-uniform surface morphology. The PA coating optical images show that low-aggregate particles covered the steel

surface when treated with phytic acid without SA. When SA was added to the phytic acid conversion bath, the size of the particles became finer, as seen in Fig.5b PA-SA-4. The coating exhibits a uniform coverage and the roughness of coating is considerably reduced with the addition of sodium alginate. The surface of PA-SA-4 is almost smooth without cracks or defects. A more smooth and homogenous surface is observed in the PA-SA-4 sample than in the PA sample. And the Ra and Rmax values were decreased to 116.4 and 228.3 nm, respectively. These observations are consistent with the thickness analysis.

One important outcome of using conversion coatings on steel substrates is to enhance the organic coating adhesion to the substrate. The composition and texture of the conversion coating can affect the surface free energy of the steel surface. When the surface free energy of coating is increased, the adhesion of the coating to the substrate and subsequent coatings is correspondingly enhanced [29]. In consequence, it was very important to evaluate the variation of the surface energy of the substrate after adding SA to the phytic acid coating. The surface chemistry of the bare steel, PA and PA-SA-4 coatings was investigated using static contact angle measurements.

We can calculate the surface free energy and work of adhesion values (W_A) according to the equations of Neumann (Eq.1) and Young (Eq.2) [30]:

$$W_A = \gamma_{1V}(1 + \cos\theta) \quad (1)$$
$$W_A = 2(\gamma_{1v} \cdot \gamma_{sv})^{1/2}\exp[-\beta(\gamma_{1v} - \gamma_{sv})^2] \quad (2)$$

In Eq.1 and 2, the variables θ and γ_{sv} are the contact angle of sample and the surface free energy of the substrate, respectively. Constant γ_{lv} is the surface tension of water (72.0 mJ/m^2) and β is 0.0001247 ± 0.000010 (mJ/m^2)^2. The calculated results are listed in Table 3 and Fig.6.

Table 3. Contact angle, work of adhesion and surface free energy values of different sample

Sample	$\Theta(°)$	W_A(mJ/m^2)	γ_{sv} (mJ/m^2)
Bare steel	71.5±1.8	94.8	40.8
PA coating	35.6±2.3	130.5	59.4
PA-SA-4 coating	19.2±3.1	140.0	64.3
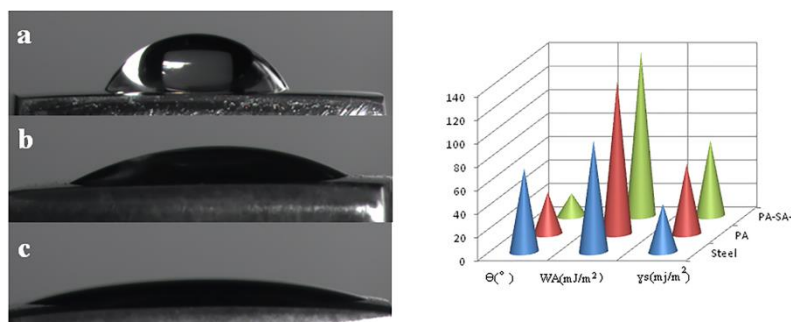
Figure 6. Contact angle diagram of different samples and the relationship between contact angle, surface free energy and work of adhesion values

The contact angle of the untreated steel substrate was approximately 71.5±1.8°, indicating substantial hydrophilic properties. Fig.6 demonstrates that the deposition of phytic acid on the steel surface compared to the untreated steel decreased the contact angle. The results also show the increase in γ_{sv} and W_A of the coated samples after treatment by PA. The decreased contact angle after PA deposition is attributed to the phosphate groups that bear two hydroxyl groups and four hydrogen atoms. On the other hand, the sodium alginate chelation filled and sealed the cracks of the PA coating and provided a smooth surface with excellent wettability. The hydrophilic nature of SA enables strong adhesion [31]. The lowest contact angle is observed in the PA-SA-4 sample. The addition of SA to the phytic acid bath results in smaller contact angle and higher surface free energy value than without the SA additive. The change in surface morphology combined with the higher surface free energy of the surface improves the coating wettability of the metal surface. These observations indicate that incorporation of SA into the PA solution does not degrade the hydrophilicity of the coating deposited on the steel.

3.2 Corrosion resistance assessment

3.2.1 Electrochemical impedance spectroscopy measurements

The anticorrosion performances of the bare steel, PA bath treated and PA bath contain different concentrations SA treated samples was evaluated by EIS and polarization measurements. The EIS analysis was carried out on different coated samples dipped in 3.5 wt% NaCl solution. The electrochemical impedance spectra of the different coated samples are presented in Fig.7.
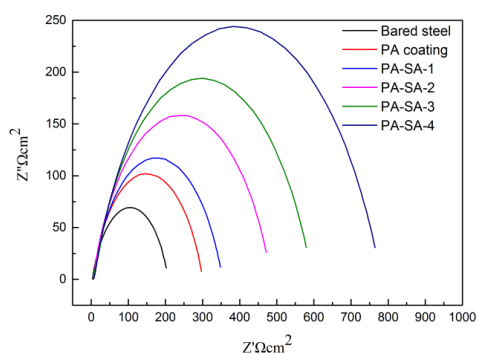
Figure 7. Impedance diagrams of samples treated with different conversion baths

According to the characteristics of the impedance spectra, the equivalent circuit for studies are shown in Fig.8.
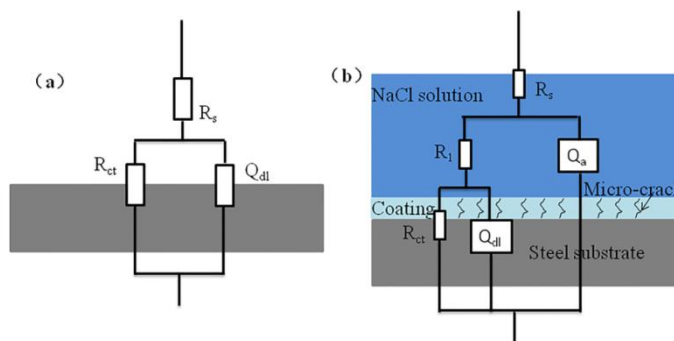
Figure 8. The equivalent circuit models for data fitting

In this equivalent circuit, R_s is the resistance of the electrolyte resulting from the ohmic or uncompensated resistance of the solution between the working electrodes and reference electrodes. R_1 and Q_a are the resistance and capacitance, respectively, of the micro-pores in the coating formed on the surface of the steel [32]. Q_{dl} is a constant phase element (CPE) that was included in the fitting instead of an ideal capacitor to simulate the double-layer capacitance at the steel/solution interface. R_{ct} is the charge transfer resistance at the interface between electrolyte and iron substrate at the crack location of the coating, which is in parallel with the double-layer capacitance at the steel/solution interface.

To quantitatively evaluate the corrosion inhibition effect of the coating, ZSimpWin software was used to simulate and analyse the EIS spectrograms. The parameters of different samples obtained from the fitting parameters of the experimental impedance spectra are summarized in Table 4.

Table 4. EIS spectra fitting parameters of different coated samples

Sample	$R_S/(\Omega \cdot cm^2)$	$R_1/(\Omega \cdot cm^2)$	$Q_a/\mu Fcm^2$	$R_{ct}/(\Omega \cdot cm^2)$	$Q_{dl}/\mu Fcm^2$
Bare steel	3.898	/	/	170.3	645.4
PA coating	4.685	22.1	532.0	273.6	64.6
PA-SA -1	4.551	33.5	514.6	315.8	73.3
PA-SA -2	3.915	40.3	506.2	440.9	43.6
PA-SA -3	4.481	48.4	453.6	490.1	57.6
PA-SA -4	6.694	52.3	315.5	742.9	11.9

Fig. 7 shows the impedance as a single semicircle, the radius of which enlarges with increased SA concentration. This demonstrates that the corrosion reaction charge transfer resistance increases and the corrosion rate decreases. The PA-SA-4 coating exhibited a better corrosion resistance than the phytic acid coating. The data presented in Table 4 suggest that the coating resistance and charge transfer resistance increase with increasing SA concentration, indicating that the sample treated with PA-SA had a higher corrosion resistance to corrosive ions. This increase is consistent with the reduced porosity seen when SA was added to the treatment solution. In general, a metal surface coating that performs well in corrosion protection is characterized by a higher charge transfer resistance [33].

Notably, the R_{ct} value of the PA-SA-4 sample is approximately five times that of bare steel, suggesting that the corrosion process is effectively impeded.

3.2.2 Polarization measurements

The polarization measurement was also tested on the coated samples to investigate the corrosion protection mechanism.

Polarization curves of different conversion coating are presented in Fig.9. The electrochemical corrosion kinetic parameters such as polarization resistance (R_p), corrosion current density (I_{corr}) and corrosion potential (E_{corr}), obtained by extrapolation of Tafel lines are summarized in Table 5.
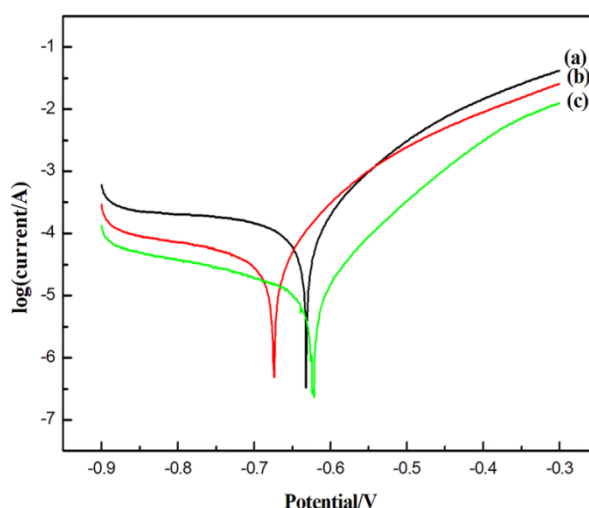
Figure 9. Polarization plots of a) bare steel, b) phytic acid coating, c) PA-SA-4

Table 5. Polarization parameters for the samples exposed to 3.5 wt% NaCl solution

Sample	I_{corr} ($\mu A/cm^2$)	E_{corr} (V vc.SCE)	R_p (Ωcm^2)	P (%)
Bare steel	142.6	-0.632	238.3	—
PA coating	49.57	-0.674	642	38.5
PA-SA-4	15.07	-0.622	1874	12.6

Can be seen from the Fig. 9 and Table 5, steel samples treated with phytic acid solution and the enhancement increase when adding SA resulted in a lower corrosion current density (I_{corr}) and a higher polarization resistance (R_p) compared to the untreated steel sample. The PA-SA treated coating showeded a corrosion current density more than 3 and 10 times lower than phytic acid coating and bare steel, respectively. Moreover, the polarization resistance of the steel coated in the presence of SA was approximately three times larger than that when using phytic acid alone. The findings indicate that the corrosion rate of the steel samples was significantly reduced by the conversion coatings.

The deposition of phytic acid resulted in the corrosion potential (E$_{corr}$) being shifted towards a more negative value compared to the bare steel, indicating that the phytic acid coating affected the cathodic reaction more intensely than anodic reaction. The SA-containing phytic acid coating also affected both the anodic and cathodic branches. The cathodic and anodic current of the PA-SA conversion coating is lower than that of the bare steel and phytic acid coated sample, meaning that both the cathodic and anodic branches were suppressed and it significantly increases the corrosion resistance of the steel sample. Simultaneously, the cathodic reaction was markedly retarded via arresting the reduction of water, which was transported mainly through the open pores of the coating. Since the reduction of water was prevented, which was transported mainly through the cracks of the coating, the cathodic reaction was significantly retarded. However, the corrosion potential (E$_{corr}$) shifted towards a more positive direction (from -0.632V to -0.622V) compared to that when using the phytic acid coating. This finding demonstrates that SA enhanced the anticorrosion performance of the phytic acid coating through further blocking the transport of corrosive ions to the active sites, particularly the anodic sites on the steel surface. Added SA to phytic acid conversion bath can provide much better protection against corrosion. And this is consistent with the results of electrochemical impedance result.

4.DISCUSSION

The electrochemical measurement results have demonstrated that incorporated SA into the phytic acid coating bath resulted in a markedly improvement of the anticorrosion performance of phytic acid based conversion coating. Additionally, incorporated SA into the phytic acid treatment bath changed the structure and morphology of the prepared phytic acid based coating.

The precipitation of phytic acid coating on the steel surface in the absence of the SA can be explained by the following reaction:

$$Fe \rightarrow Fe^{2+} + 2e^-$$

$$RH_{10}^{2-} + Fe^{2+} \rightarrow FeRH_{10}$$

$$RH_{10}^{2-} + H_2O \rightarrow RH_9^{3-} + H_3O^+$$

$$RH_9^{3-} + Fe^{3+} \rightarrow FeRH_9$$

$$R = C_6H_6O_6(PO_3)_6$$
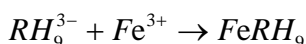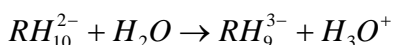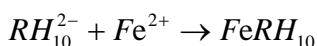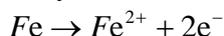
The active groups of phytic acid can react with Fe^{2+}/Fe^{3+} in the conversion bath to form chelate compounds, which are then deposited on the steel surface. The SEM/EDS and AFM analyses showed that the addition of SA to the phytic acid conversion bath vanished the crack. Added the SA to the phytic acid conversion bath, the porosity of prepared phytic acid coating was decreased.The phytic acid conversion coating is mainly composed of phytic acid complexes. Pores in the conversion coating can be regarded as areas of exposed substrate. Using electrochemical methods such as EIS and polarization, the coating porosity P(%) can be evaluated according to Eq.3[34]:

$$P = \frac{R_{PS}}{R_P} \times 10^{-\left(\frac{\Delta E_{corr}}{\beta a}\right)} \quad (3)$$

Where P is the porosity of the conversion coating, R_{ps} and R_p are the polarization resistance of the untreated sample and the conversion coating, respectively. E_{corr} is the potential difference between the untreated and conversion bath treated steel. βα is the the anodic Tafel coefficient of the untreated steel. The P(%) value represents the percentage of the active area on the conversion coating. The P(%) values of 38.5 and 12.6 were calculated for the phytic acid coatings in the absence and presence of SA, respectively. After the addition of SA, the P(%) values of the PA-SA coated sample decreased from 38.5 to 12.6, which is one-third of the porosity of the phytic acid coating. However, due to its large molecular volume, the sodium alginate cannot fill all of the cracks in the PA coating. Therefore, the P(%) is still quite high. It is probable that the carboxylic group (COO−) present on the polymeric backbone of SA chelated with multivalent cations such as Fe^{2+} and Fe^{3+} on the steel surface to form complexes [35]. This rationale is schematically illustrated in Fig.9. SA includes many COOH groups, which highly tend to be adsorbed onto the steel surface, retarding the dissolution rate of the steel. All of these observations reveal that SA was able to enhance the anticorrosion resistance of the phytic acid based conversion coating through two central mechanisms. First of all, SA increased the phytic acid coating barrier performance by reducing the porosity of the coating. Secondly, the SA was adsorbed and formed a protective film on the steel surface, thus restricting steel dissolution.
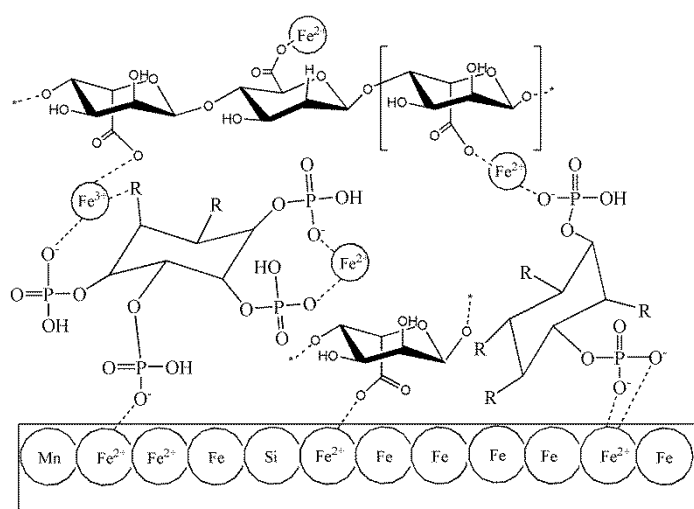
Figure 9. Schematic of phytic acid and SA chelation with metal ions to form conversion coating

5. CONCLUSIONS

Sodium alginate was added to the phytic acid conversion bath and the effects of this green chelating agent on the morphology and chemical properties of the phytic acid based conversion coating were studied on the steel surface. The results showed that the steel coated with phytic acid in the presence of SA had better corrosion resistance and lower porosity. The corrosion protective efficiency of the phytic acid conversion coating increased with the increase of SA concentration. The SEM, XPS

and AFM results indicated that phytic acid could deposit on the steel surface to form a protective film. Simultaneously, the coating adhesion to the top layer did not decrease with the addition of SA. The phytic acid coatings proposed in this study would constitute a first line treatment (primer) on the steel surface with the aim of reducing micro-cracks and improving corrosion resistance. Increasing attention will be given to not only improving the protective efficiency of the conversion coating, but also to endow it with self-repairing capabilities and a final top coat will be crucial to obtain adequate corrosion protection.

ABOUT THE AUTHORS
First author: Yong Lu; doctor from LanzhouUniversityofTechnology. The author's area of research is the application of functional materials in the field of anti-corrosion. Second author: Huixia Feng, professor, doctoral supervisor from LanzhouUniversityofTechnology. The author's area of research is the application of functional composite materials.

CONFLICTS OF INTEREST
The authors confirm that this article content has no conflicts of interest.

ACKNOWLEDGEMENTS

References

1. F. Crea, C.D. Stefano, D. Milea and S. Sammartano, *Coord. Chem. Rev.*,252 (2008) 13.
2. J. Winiarski, J. Masalski and B. Szczygieł, *Surf. Coat. Technol.*, 236 (2013) 252.
3. M. Motamedi and M.M. Attar, *RSC Adv.*, 6 (2016) 44732.
4. E. Legghe, E. Aragon, L. Bélec, A. Margaillan and D. Melot, *Prog. Org. Coat*, 66 (2009) 5.
5. X. Gao, W. Li, R. Yan, H. Tian and H. Ma, *Surf. Coat. Technol.*, 325 (2017) 248.
6. R. Yan, X. Gao, W. He, R. Guo, R. Wu, Z. Zhao and H. Ma, *RSC Adv.*, 7 (2017) 41152.
7. M. Tamilselvi, P. Kamaraj, M. Arthanareeswari, S. Devikala and J. A. Selvi, *Appl. Surf . Sci.*, 332 (2015) 12.
8. C. Jiang, Y. Cao, G. Xiao, R. Zhu and Y. Lu, *RSC Adv.*, 7 (2017) 7531.
9. B. Ramezanzadeh, H. Vakili and R. Amini, *Appl. Surf Sci.*, 327 (2015) 174.
10. E. Saei, B. Ramezanzadeh, R. Amini and M. S. Kalajahi, *Corros. Sci.*, 127 (2017) 186.
11. G. Kong, L.Y. Ling, J. Lu, C. Che and Z. Zhong, *Corros. Sci.*, 53 (2011) 1621.
12. H. Hassannejad, M. Moghaddasi, E. Saebnoori and A.R. Baboukani, *J. Alloys Compd.*, 725 (2017) 968.
13. H. Zhao, S. Cai, Z. Ding, M. Zhang, Y. Li and G. Xu, *RSC Adv.*, 5 (2015) 24586.
14. R. Maurya, A.R. Siddiqui and K. Balani, *Appl. Surf . Sci.*, 443 (2018) 429.
15. X. Gao, K. Lu, L. Xu, H. Xu, H. Lu, F. Gao, S. Hou and H. Ma, *Nanoscale,* 8 (2016) 1555.
16. A.D. Nicolò, L. Paussa, A. Gobessi, A. Lanzutti, C. Cepek, F. Andreatta and L. Fedrizzi, *Surf. Coat. Technol.*, 287 (2016) 33.
17. L.A. Hernandez-Alvarado, L.S. Hernandez and S.L. Rodriguez-Reyna, *Int. J. Corros.*, 2012 (2012) 1.
18. H.F. Gao, H.Q. Tan, J. Li, Y.Q. Wang and J.Q. Xun, *Surf. Coat. Technol.*, 212 (2012) 32.
19. R. Zhang, S. Cai, G. Xu, H. Zhao, Y. Li, X. Wang, K. Huang, M. Ren and X. Wu, *Appl. Surf. Sci.,* 313 (2014) 896.
20. L. Diaz, F. R. García-Galván, I. Llorente, A. Jiménez-Morales, J.C. Galván and S.J. Feliu, *RSC*

Adv., 5 (2015) 105735.
21. R. M. Hassan and I. A. Zaafarany, *Materials*, 6 (2013) 2436.
22. P. Zhang, Q. Li, L.Q. Li, X.X. Zhang and Z.W. Wang, *Mater. Corros.*, 66 (2015) 31.
23. I.B. Obot, I.B. Onyeachu and A.M. Kumar, *Carbohydr. Polym.*, 178 (2017) 200.
24. Y. Sangeetha, S. Meenakshi and S.C. Sairam, *J. Appl. Polym. Sci.*, 133 (2016) 6.
25. N. Nagasawa, H. Mitomo, F. Yoshii and T. Kume, *Polym. Degrad. Stab.*, 69 (2000) 9.
26. H. Shi, E.H. Han, F. Liu and S. Kallip, *Appl. Surf. Sci*, 280 (2013) 325.
27. X. Chen, G. Zeng, T. Gao, Z. Jin, Y. Zhang, H. Yuan and D. Xiao, *Electrochem. Commun*, 74 (2017) 42.
28. S.K. Papageorgiou, E.P. Kouvelos, E.P. Favvas, A.A. Sapalidis, G.E. Romanos and F.K. Katsaros, *Carbohydr. Res.,* 345 (2010) 469.
29. B. Ramezanzadeh, M. Akbarian, M. Ramezanzadeh, M. Mahdavian, E. Alibakhshi and P. Kardar, *J Electrochem. Soc.*, 6 (2012) 7.
30. D. Li and A. Neumann. *J. Colloid. Interface Sci.,* 137 (1990) 4.
31. M. Rajkumar, N. Meenakshisundaram and V. Rajendran, *Mater. Charact.*, 62 (2011) 11.
32. N. Dang, Y.H. Wei, L.F. Hou, Y.G. Li and C.L. Guo, *Mater. Corros.*, 66 (2015) 1354.
33. M. Garcia-Heras, A. Jimenez-Morales, B. Casal, J.C. Galvan, S. Radzki and M.A. Villegas, *J. Alloys Compd.*, 380 (2004) 6.
34. F.C. Lins, G.F.A. Reis, C.R. Araujo and T. Matencio, *Appl. Surf. Sci.*, 205 (2006) 10.
35. L. Sang, J. Huang, D. Luo, Z. Chen and X. Li, *J. Mater. Sci. :Mater. Med.*, 21 (2010) 2561.